Asian Journal of Chemistry; Vol. 37, No. 1 (2025), 166-176

ASIAN JOURNAL OF CHEMISTRY

https://doi.org/10.14233/ajchem.2025.32973

Design, Synthesis and *in silico* Study of Diarylsulfide Piperazine-Amide Hybrids as Antibacterial Motifs

K. Sajitha[1], V.V.P.C. Narayana[1], V. Bala Yesu[1,2], D.M. Manjunath[3], P. Suresh Yadav[4], K. Vamsi[5], D. Suresh Babu[1], V. Murali[1], A.M. Uttam[6], A. Anitha[2], J. Bhanu Prasad[2], M. Chandra Subhash[4], D. Srinivasulu[1] and N.V.V. Jyothi[1,*]

[1]Department of Chemistry, Sri Venkateswara University, Tirupati-517502, India
[2]SGK Government Degree College, Vinukonda, Palnadu-522647, India
[3]Department of Plant Sciences, School of Life Sciences, University of Hyderabad, Gachibowli-500046, India
[4]Department of Microbiology, Yogi Vemana University, Kadapa-516005, India
[5]Indian Institute of Science Education and Research (IISER) Tirupati-517507, India
[6]Department of Pharmaceutical Chemistry, Shree Dhanvantary Pharmacy College, Kim, Suram-394110, India

*Corresponding author: E-mail: nvvjyothi73@gmail.com

Received: 31 October 2024; *Accepted*: 12 December 2024; *Published online*: 31 December 2024; AJC-21864

Novel antimicrobial drugs are required to fight the serious global health challenge of antibiotic resistance. In this study, 12 hybrids of diarylsulfide (DAS) piperazine-amide **8a-l** were synthesized. All the 12 compounds were assessed for the antibacterial study against Gram-positive and Gram-negative bacteria. Antibacterial structure-activity relationship (SAR) analysis revealed that disubstituted compounds, particularly **8h** (3,4-dinitro) and **8j** (2,4-dichloro), exhibited superior antibacterial activity and also states that *ortho*-substituted compounds performing better than *para*-substituted ones. Molecular docking studies further strengthened antibacterial efficacy of disubstituted compounds **8h** (-7.58 kcal/mol) and **8j** (7.14 kcal/mol) exhibited the highest binding affinity to the DNA gyr. A enzyme, interacting with essential residues critical for bacterial DNA replication. It was concluded that strong binding, alongside favourable lower RMSD values, allows these compounds to effectively inhibit DNA gyrase. Therefore, these DAS piperazine-amide compounds represent promising lead compounds for further study as antibacterial agents.

Keywords: Diarylsulfide, Piperazine-amide, Antibiotic resistance, Antibacterial efficacy, DNA enzyme.

INTRODUCTION

The fight against bacterial infections heavily relies on the development of effective antibacterial agents that inhibit the proliferation of bacteria while minimizing toxicity to surrounding tissues. Recent advances in antimicrobial medicines, including β-lactams, carbapenems and cephalosporins, have involved chemically modifying naturally occurring substances to enhance their efficacy [1-3]. Synthetic antibiotics, such as aminoglycosides, further contribute to this arsenal, with compounds classified as either bactericidal (killing bacteria) or bacteriostatic (inhibiting their growth) [4]. However, the emergence of bacterial resistance, exacerbated by the overuse and misuse of these drugs, poses a significant challenge to public health and the pharmaceutical industry. The World Health Organization (WHO) has underscored the urgency of addressing antimicrobial resistance (AMR), particularly in light of the COVID-19 pandemic. As bacteria, fungi and viruses evolve, the need for innovative strategies in drug design becomes increasingly critical [5,6].

Researchers are using the hybrid drug strategy to develop new antimicrobial agents to combat drug resistance. This involves combining chemical fragments, linked *via* cleavable or non-cleavable teethers, to create heteromeric molecules with biological activity. This approach integrates chemical synthesis, pharmacology and microbiology to enhance antimicrobial efficacy [7]. In this connection, heterocyclic compounds play a crucial role in medicinal chemistry, forming the backbone of many biologically active natural products and synthetic drugs. Their versatile structures are often linked to various biological functions, making them highly valued in drug design. In 2021, nine out of twelve drugs approved by the US-FDA featured

heterocyclic scaffolds as key pharmacophores, underscoring their significance in contemporary pharmacology [8].

Among these hybrids, diarylsulfides (DASs) are noteworthy as versatile intermediates in various biologically active compounds and materials (Fig. 1). These thioether analogues have shown potential against numerous health issues, including cancer, HIV and neurodegenerative diseases. Notable DAS-derived drugs include antitumor and antibacterial agents, emphasizing their broad therapeutic applications [9-12]. In addition, piperazine derivatives represent a diverse group of compounds characterized by a core heterocyclic piperazine structure, where minor alterations in substitution patterns can significantly impact their biological activity. Recent research has highlighted their antibacterial properties, along with a wide array of other biological functions. These compounds serve as crucial building blocks in drug discovery, showing promising results across various biological screens. Their versatility extends to antiviral, antimicrobial, anti-inflammatory, anticancer, antiischemic, antimycobacterial, antiparasitic, anticonvulsant and antituberculosis activities, as well as inhibition of acetylcholinesterase. This broad spectrum of biological effects underscores the potential of piperazine derivatives in developing new therapeutic agents [13-16].

Minor structural modifications can drastically alter their antibacterial properties, leading to the synthesis of a wide range of active compounds. The exploration of sulfides and amides also reveals promising antibacterial and enzyme inhibitory activities. Moreover, sulfides and amides have shown considerable promise in biological activities, particularly in antibacterial and enzyme inhibition contexts. DNA gyrase, a crucial topoisomerase II enzyme in bacteria, is essential for DNA transcription, replication and chromosome segregation. Comprising two subunits Gyrase-A and Gyrase-B this enzyme catalyzes DNA breakage and rejoining, facilitating negative supercoiling vital for bacterial survival. Targeting DNA gyrase and topoisomerase IV represents a promising strategy in antibacterial drug development, as inhibition of these enzymes disrupts DNA synthesis and leads to bacterial cell death [17]. Given their absence in higher eukaryotes, these targets are particularly attractive for developing novel antibacterial agents.

Hence, in this study, we synthesized and characterized a new class of diarylsulfide piperazine-amide derivatives, utilizing diarylsulfide core as a foundational structure. By incorporating various amide moieties into the piperazine framework, we enhanced the diversity of these compounds and increased their binding potential with biological targets. The synthesized derivatives underwent *in vitro* evaluation to assess their antibacterial efficacy against a range of bacterial strains. Furthermore, we confirmed the findings by computer docking investigations, which elucidated the binding relationships and modes of action of these new drugs. This comprehensive approach contributed to the development of effective antibacterial agents in the ongoing fight against antimicrobial resistance.

EXPERIMENTAL

Chemicals were obtained from suppliers and used without purification. The progress of the reaction was monitored using TLC and compounds were purified through column chromatography using silica gel (60-120 mesh). FT-IR spectra were recorded using a Shimadzu-8400 spectrometer. The ^{1}H NMR and ^{13}C NMR spectra were recorded using Bruker-500 spectrometers. Tetramethylsilane was used an the internal standard, with data reported in parts per million (δ, ppm) and hertz (J = Hz). The HR-MS analysis was performed using a Xevo TQD quadrupole mass spectrometer.

General methods of synthesis of DAS-piperazine-amide analogues

General procedure of synthesis of (2-nitrophenyl)-(phenyl)sulfane (2): Thiophenol (**1**, 72 mmol), 1-chloro-2-nitrobenzene (72 mmol) and anhydrous K_2CO_3 (108 mmol) were refluxed in acetonitrile (80 mL) for 8 h. After completing the reaction, the reaction crude was allowed to cool, the mixture was filtered to give desired compound **2** as solid after recrystallization with methanol.

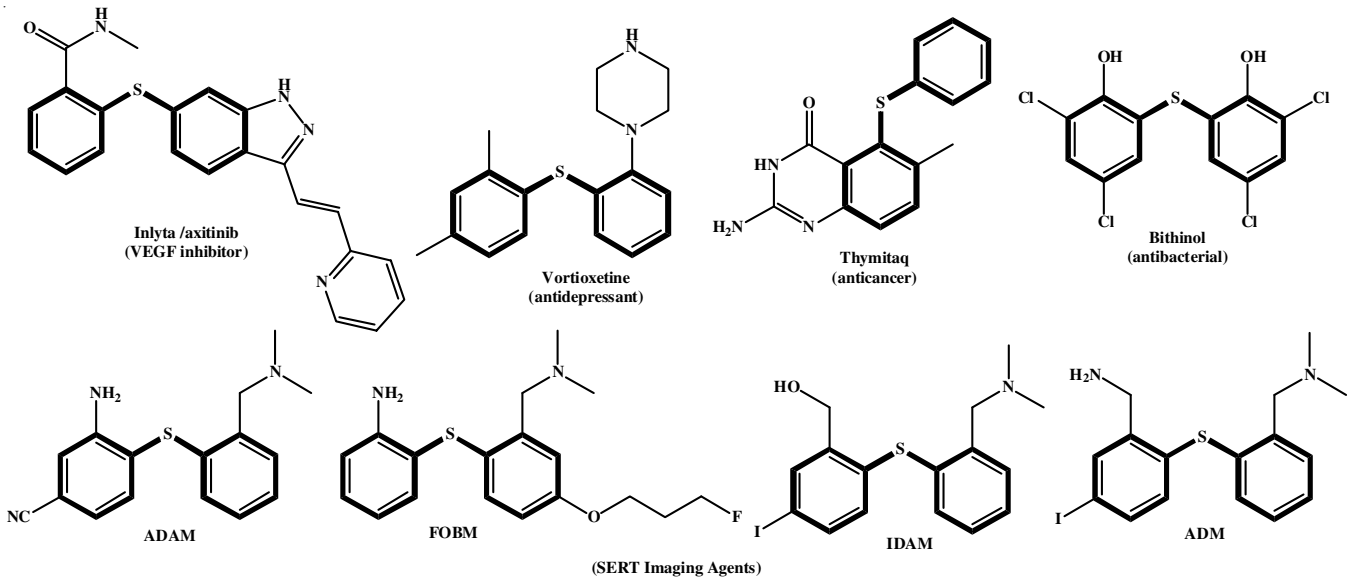

Fig. 1. Some biologically active diarylsulfide (DAS) derivatives

General procedure of synthesis of 2-(phenylthio)-aniline (3): A mixture of compound **2** (58 mmol) and 5% of Pd/C in CH_3OH (75 mL) was placed in a three-necked round-bottomed flask and stirred at 30 ºC for 6 h. The reaction progress was monitored using TLC. After completion, the mixture was filtered through a celite pad and the filter cake was washed with methanol (15 mL). The combined filtrate was concentrated under vacuum to obtain compound **3**.

General procedure of synthesis of 2-chloro-*N*-(2-(phenylthio)phenyl)acetamide (4): A solution of compound **3** (10 mmol) and triethylamine (20 mmol) in THF (20 mL) was cooled to 0 ºC, then chloroacetyl chloride (12 mmol) was added dropwise to the solution and stirred at room temperature for 1.5 h. The mixture was then concentrated under vacuum and the crude product was extracted with water and ethyl acetate. Subsequently, the organic layer was washed with saturated $NaHCO_3$ and brine followed by dried over with anhydrous Na_2SO_4 and compound **4** was purified by using column chromatography after removing the organic solvent under vacuum.

General procedure of synthesis of *tert*-butyl-4-(2-oxo-2-((2-(phenylthio)phenyl)amino)ethyl)piperazine-1-carboxylate (5): Compound **4** (10 mmol), *N*-Boc piperazine (15 mmol), K_2CO_3 (20 mmol), KI (0.01 mmol) and 30 mL of CH_3CN were refluxed for 2 h. After completion, the solution was diluted with water and extracted using EtOAc (3 × 15 mL). The organic layer was washed with saturated $NaHCO_3$, brine, followed by saturated NH_4Cl (to remove unaltered N-Boc-piperazine) and dried over with anhydrous Na_2SO_4. Compound **5** was purified by using column chromatography after removing the organic solvent under vacuum.

General procedure of synthesis of *N*-(2-(phenylthio)-phenyl)-2-(piperazin-1-yl)acetamide (6): Compound **5** (10 mmol) and TFA (20 mmol) was suspended in 20 mL of DCM at ambient temperature and stirred for 2 h. After completion, the crude was concentrated. The substance was dissolved in 5 mL of water, saturated Na_2CO_3 solution was used to control the pH 8-9. The aqueous layer was extracted with DCM (3 × 10 mL) and organic layer was washed with saturated $NaHCO_3$, brine followed by water. Then dried over with anhydrous Na_2SO_4. The organic layer was concentrated under vacuum and purified by using column chromatography to yield residue **6** as a pale-yellow solid.

General procedure of synthesis of 2-(4-benzoylpiperazin-1-yl)-*N*-(2-(phenylthio)phenyl)acetamide (8a-l): To an ice-cooled solution of compound **6** (10 mmol) in 5 mL of DMF, appropriate aromatic carboxylic acids **7a-l** (12 mmol), hydroxybenzotriazole (HOBt) (15 mmol), (3-dimethylaminopropyl)-ethylcarbodiimide hydrochloride (EDC·HCl) (20 mmol) and a few drops of N,N-diisopropylethylamine (DIPEA) were added. The mixture was stirred at room temperature for 1 h. Subsequently, the reaction mixture was poured onto crushed ice. The resulting precipitate was filtered, dried and recrystallized from ethanol to yield title products **8a-l** (**Scheme-I**).

2-(4-(4-Chlorobenzoyl)piperazin-1-yl)-*N*-(2-(phenylthio)phenyl)acetamide (8a): White solid, yield: 68%; m.p.: 183-185 ºC, IR (KBr, ν_{max}, cm^{-1}): 3236, 2998, 1698, 1523, 1309, 1262, 1213, 115; ^1H NMR ($CDCl_3$, δ) ppm: 10.19 (s, 1H), 8.46-8.43 (m, 2H), 7.63-7.61 (m 1H), 7.56-7.48 (m, 2H), 7.41-7.38 (m, 4H), 7.41-7.38 (m, 2H), 7.33-7.30 (m, 2H), 7.23-7.17 (m, 2H), 7.05-7.00 (m, 2H), 3.53-3.31 (m, 4H), 3.11 (s, 2H), 2.52-2.35 (m, 4 H); ^{13}C NMR ($CDCl_3$, δ) ppm: 170.06, 170.04, 140.33, 137.05, 135.67, 135.5, 134.19, 129.71, 129.36,129.36, 129.08, 128.97, 128.77, 127.70, 124.55, 123.08, 121.01, 59.77, 52.73, 45.71; m.f.: $C_{25}H_{24}ClN_3O_2S$; calcd. m.w.: 466.00; HRMS: 466.1370 $[M+H]^+$.

2-(4-(4-Bromobenzoyl)piperazin-1-yl)-*N*-(2-(phenylthio)phenyl)acetamide (8b): Pale yellow solid, yield: 59%; m.p.: 182-184 ºC; IR (KBr, ν_{max}, cm^{-1}): 3236, 2998, 1698, 1523, 1309, 1262, 1213, 1155; ^1H NMR ($CDCl_3$, δ) ppm: 10.19 (s, 1H), 8.45-8.42 (m, 1H), 7.97-7.93 (m, 1H), 7.67-7.65 (m, 2H), 7.63-7.60 (m, 1H), 7.55-7.51 (m, 1H), 7.33-7.29 (m, 4H), 7.23-7.16 (m, 2H), 7.07-7.05 (m, 1H), 3.48-3.30 (m, 4H), 3.10 (s, 2H), 2.58-2.50 (m, 4H); ^{13}C NMR ($CDCl_3$, δ) ppm: 170.07, 170.06, 140.33, 135.67, 134.19, 132.34, 130.03, 129.36, 129.08, 128.77, 127.70, 125.22, 124.55, 123.08, 121.01, 59.77, 52.73, 45.71; m.f.: $C_{25}H_{24}BrN_3O_2S$; calcd. m.w.: 510.45; HRMS: 510.0864 $[M+H]^+$, 512.0846 $[M+2]^+$.

2-(4-(3,4-Dimethoxybenzoyl)piperazin-1-yl)-*N*-(2-(phenylthio)phenyl)acetamide (8c): Pale green solid, yield: 62%; m.p.: 179-184 ºC; IR (KBr, ν_{max}, cm^{-1}): 3326, 2998, 1698, 1523, 1309,1262, 1213, 1155; ^1H NMR ($CDCl_3$, δ) ppm: 10.21 (s, 1H), 8.46-8.44 (m, 1H), 8.20-8.17 (m, 1H), 7.99-7.89 (m, 1H), 7.73-7.53 (m, 4H), 7.33-7.27 (m, 2H), 7.22-7.19 (m, 2H), 7.08-6.99 (m, 1H), 6.95-6.91 (m, 2H), 3.79 (s, 6H), 3.49-3.26 (m, 4H), 3.13 (s, 2H), 2.47-2.34 (m, 4H); ^{13}C NMR ($CDCl_3$, δ) ppm: 170.06, 169.29, 153.03, 148.24, 140.33, 135.67, 134.19, 129.65, 129.36, 129.08, 128.77, 127.70, 124.55, 123.47, 123.08, 121.01, 113.08, 110.71, 59.77, 55.98, 55.94, 52.73, 45.78; m.f.: $C_{29}H_{29}N_3O_4S$; Calcd. m.w.: 491.61; HRMS: 492.1963 $[M+H]^+$.

2-(4-(4-Nitrobenzoyl)piperazin-1-yl)-*N*-(2-(phenylthio)phenyl)acetamide (8d): Pale yellow solid, yield: 64%; m.p.: 187-191 ºC; IR (KBr, ν_{max}, cm^{-1}): 3326, 2998, 1698, 1523, 1309,1262, 1212, 1155; ^1H NMR ($CDCl_3$, δ) ppm: 10.19 (s, 1H), 8.45-8.43 (m, 1H), 7.64-7.62 (m, 1H), 7.57-7.49 (m, 4H), 7.40-7.37 (m, 2H), 7.35-7.33 (m, 2H), 7.26-7.15 (m, 2H), 7.09-7.05 (m, 2H), 3.52-3.30 (m, 4H), 3.12 (s, 2H), 2.53-2.34 (m, 4H); ^{13}C NMR ($CDCl_3$, δ) ppm: 170.07, 148.42, 142.29, 140.33, 135.67, 134.19, 129.36, 129.08, 128.77, 127.95, 127.70, 124.55, 123.24, 123.08, 121.01, 59.77, 52.73, 45.71; m.f.: $C_{25}H_{24}N_4O_4S$; Calcd. m.w.: 476.55; HRMS: 477.6827 $[M+H]^+$.

2-(4-(4-Fluorobenzoyl)piperazin-1-yl)-*N*-(2-(phenylthio)phenyl)acetamide (8e): Pale yellow solid; yield: 64%; m.p.: 174-176 ºC; IR (KBr, ν_{max}, cm^{-1}): 3236, 2998, 1698, 1523, 1309, 1262, 1212, 1155; ^1H NMR ($CDCl_3$, δ) ppm: 10.20 (s, 1H), 8.45-8.43 (m, 1H), 7.64-7.61 (m, 1H), 7.56-7.52 (m, 1H), 7.45-7.41 (m, 2H), 7.37-7.27 (m, 5H), 7.23-7.17 (m, 2H), 7.08-7.05 (m, 1H), 3.53-3.30 (m, 4H), 3.13 (s, 2H), 2.53-2.34 (m, 4H); ^{13}C NMR ($CDCl_3$, δ) ppm: 170.15, 170.06, 165.82, 163.84, 140.33, 135.67, 134.19, 133.05, 133.02, 130.65, 130.58, 129.36, 129.08, 128.77, 127.70, 124.55, 123.08, 121.01, 115.89, 115.71, 59.77, 52.73, 45.71; m.f.: $C_{25}H_{24}FN_3O_2S$: calcd. m.w.: 449.57; HRMS: 450.1662 $[M+H]^+$.

2-(4-(4-Hydroxy-3-methoxybenzoyl)piperazin-1-yl)-*N*-(2-(phenylthio)phenyl)acetamide (8f): Pale-green solid,

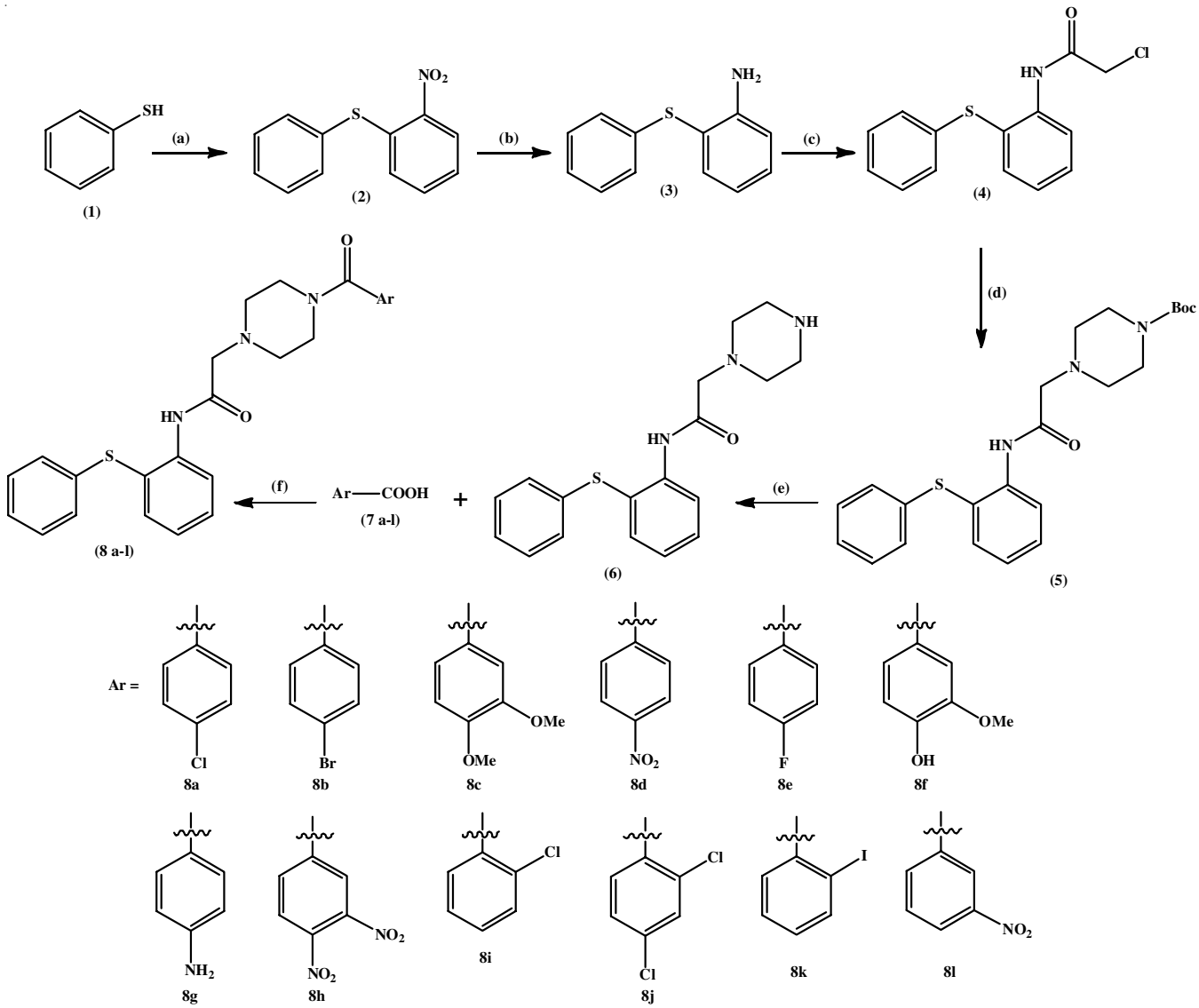

Scheme-I: Synthesis of diarylsulfide piperazine amide derivatives (**8a-l**) [Reagents and conditions: (a) 1-Chloro-2-nitrobenzene, K_2CO_3, acetonitrile, 78-82 °C; (b) Pd/C, H_2, methanol, 30 °C; (c) Chloroacetyl chloride, NEt_3 THF; d) N-Boc piperazine, K_2CO_3, KI, CH_3CN; (e) TFA, DCM, 2 h; (f) EDC·HCl, HOBt, DIPEA, DMF

yield: 61%; m.p.: 189-191 ºC; IR (KBr, ν_{max}, cm^{-1}): 3236, 2998, 1698, 1523, 1309, 1262, 1213, 1155; ^{1}H NMR ($CDCl_3$, δ) ppm: 10.19 (s, 1H), 8.45-8.43 (m, 1H), 7.59-7.57 (m, 1H), 7.56-7.51 (m, 1H), 7.51-7.45 (m, 2H), 7.37-7.27 (m, 5H), 7.23-7.17 (m, 2H), 7.08-7.05 (m, 2H), 3.78 (s, 3H), 3.48-3.29 (m, 4H), 3.13 (s, 2H), 2.50-2.38 (m, 4H); ^{13}C NMR ($CDCl_3$, δ) ppm: 170.06, 169.30, 147.68, 147.40, 140.33, 135.67, 134.19, 129.36, 129.08, 128.77, 128.36, 127.70, 124.55, 123.49, 123.08, 121.01, 115.27, 110.85, 59.77, 56.09, 52.73, 45.78; m.f.: $C_{26}H_{27}N_3O_4S$; calcd. m.w.: 477.58; HRMS: 478.1817 $[M+H]^+$.

2-(4-(4-Aminobenzoyl)piperazin-1-yl)-*N*-(2-(phenylthio)phenyl)acetamide (8g): Pale pink solid, yield: 69%; m.p.: 174-176 ºC; IR (KBr, ν_{max}, cm^{-1}): 3236, 1698, 1523, 1309, 1262, 1213, 1155; ^{1}H NMR ($CDCl_3$, δ) ppm: 10.21 (s, 1H), 8.45-8.42 (m, 1H), 7.62-7.60 (m, 1H), 7.53-7.51 (m, 2H), 7.37-7.01 (m, 9H), 6.54-6.52 (m, 2H), 5.53 (s, 2H), 3.21-3.10 (m, 4H), 2.94 (s, 2H), 2.50-2.36 (m, 4H); ^{13}C NMR ($CDCl_3$, δ) ppm: 170.16, 170.06, 152.48, 140.00, 135.67, 134.18, 130.12, 129.94, 129.36, 129.08, 128.77, 127.70, 124.55, 123.08, 121.01, 114.79, 59.77, 52.73, 45.71; m.f.: $C_{25}H_{26}N_4O_2S$; calcd. m.w.: 446.57; HRMS: 447.1859 $[M+H]^+$.

2-(4-(3,4-Dinitrobenzoyl)piperazin-1-yl)-N-(2-(phenylthio)phenyl)acetamide (8h): Pale-yellow solid, yield: 62%; m.p.: 174-176 °C; IR (KBr, ν_{max}, cm^{-1}): 3236, 1698, 1523, 1309, 1262, 1213, 1155; ^{1}H NMR ($CDCl_3$, δ) ppm: 10.19 (s, 1H), 8.46-8.43 (m, 1H), 7.63-7.61 (m, 1H), 7.56-7.48 (m, 4H), 7.40-7.37 (m, 2H), 7.35-7.33 (m, 2H), 7.25-7.16 (m, 2H), 7.08-7.05 (m, 2H), 3.49-3.28 (m, 4H), 3.08 (s, 2H), 2.52-2.38 (m, 4H); ^{13}C NMR ($CDCl_3$, δ) ppm: 170.06, 168.49, 144.34, 141.64, 140.33, 135.67, 134.19, 132.35, 129.36, 129.08, 128.77, 127.70, 126.77, 126.28, 124.55, 123.08, 121.01, 59.77, 52.73, 45.81; m.f.: $C_{25}H_{23}N_5O_6S$; calcd. m.w.: 521.55; HRMS: 522.4726 $[M+H]^+$.

2-(4-(2-Chlorobenzoyl)piperazin-1-yl)-*N*-(2-(phenylthio)phenyl)acetamide (8i): White solid, yield: 69%; m.p.: 174-176 ºC, IR (KBr, ν_{max}, cm^{-1}): 3236, 2998, 1698, 1523, 1309,

1262, 1213, 1155; ^{1}H NMR ($CDCl_3$, δ) ppm: 10.21 (s, 1H), 8.46-8.43 (m, 1H), 7.64-7.62 (m, 1H), 7.56-7.48 (m, 4H), 7.41-7.38 (m, 2H), 7.33-7.30 (m, 2H), 7.25-7.16 (m, 2H), 7.09-7.05 (m, 2H), 3.52-3.30 (m, 4H), 3.12 (s, 2H), 2.53-2.34 (m, 4H); ^{13}C NMR ($CDCl_3$, δ) ppm: 170.06, 168.77, 140.33, 135.67, 135.25, 134.19, 131.59, 131.15, 129.84, 129.36, 129.08, 128.86, 128.77, 127.70, 127.34, 124.55, 123.08, 121.01, 59.77, 52.82, 45.84; m.f.: $C_{25}H_{24}ClN_3O_2S$; calcd. m.w.: 466.00, HRMS: 467.2630 $[M+H]^+$.

2-(4-(2,4-Dichlorobenzoyl)piperazin-1-yl)-*N*-(2-(phenylthio)phenyl)acetamide (8j): White solid; yield; 58%; m.p.: 182-186 ºC; IR (KBr, ν_{max}, cm^{-1}): 3326, 2998, 1698, 1523, 1309, 1262, 1213, 1155; ^{1}H NMR ($CDCl_3$, δ) ppm: 10.18 (s, 1H), 8.45-8.43 (m, 1H), 7.64-7.62 (m, 1H), 7.57-7.49 (m, 4H), 7.40-7.37 (m, 2H), 7.35-7.33 (m, 2H), 7.25-7.16 (m, 1H), 7.09-7.05 (m, 2H), 3.52-3.34 (m, 4H), 3.14 (s, 2H), 2.53-2.34 (m, 4H); ^{13}C NMR ($CDCl_3$, δ) ppm: 170.06, 168.25, 140.33, 136.84, 135.67, 134.19, 133.80, 133.64, 130.37, 130.28, 129.36, 129.07, 128.77, 127.70, 124.55, 123.08, 121.01, 59.77, 52.85, 45.84; m.f.: $C_{25}H_{23}Cl_2N_3O_2S$; calcd. m.w.: 500.04; HRMS: 501.3257 $[M+H]^+$.

2-(4-(2-Iodobenzoyl)piperazin-1-yl)-*N*-(2-(phenylthio)-phenyl)acetamide (8k): Pale red solid, yield: 65%; m.p.: 194-196 ºC; IR (KBr, ν_{max}, cm^{-1}): 3236, 2998, 1698, 1523, 1309, 1262, 1213, 1155; ^{1}H NMR ($CDCl_3$, δ) ppm: 10.18 (s, 1H), 8.42-8.40 (m, 1H), 7.60-7.58 (m, 1H), 7.56-7.52 (m, 1H), 7.45-7.41 (m, 2H), 7.37-7.27 (m, 5H), 7.23-7.17 (m, 2H), 7.08-7.06 (m, 2H), 3.71-3.52 (m, 4H), 3.36 (s, 2H), 2.90-2.80 (m, 4H); ^{13}C NMR ($CDCl_3$, δ) ppm: 171.57, 170.27, 141.62, 139.82, 139.40, 135.67, 134.43, 130.35, 129.36, 129.23, 129.08, 128.36, 128.00, 127.70, 124.55, 122.01, 121.07, 93.92, 60.11, 52.94, 46.70; m.f.: $C_{25}H_{24}IN_3O_2S$; Cacld. m.w.: 557.45; HRMS: 558.2560 $[M+H]^+$.

2-(4-(3-Nitrobenzoyl)piperazin-1-yl)-*N*-(2-(phenylthio)-phenyl)acetamide (8l): Pale yellow solid, yield: 68%; m.p.: 194-196 ºC; IR (KBr, ν_{max}, cm^{-1}): 3236, 2998, 1698, 1523, 1309, 1262, 1212, 1155. ^{1}H NMR ($CDCl_3$, δ) ppm: 10.20 (s, 1H), 8.45-8.43 (m, 1H), 8.32-8.30 (m, 1H), 8.18-8.16 (m, 1H), 7.85-7.83 (m, 3H), 7.63-7.52 (m, 3H), 7.34-7.30 (m, 3H), 7.23-7.16 (m, 3H), 7.09-7.06 (m, 1H), 3.34-3.32 (m, 4H), 3.13 (s, 2H), 2.51-2.37 (m, 4H); ^{13}C NMR ($CDCl_3$, δ) ppm: 170.06, 168.75, 147.044, 140.33, 136.40, 135.67, 134.19, 133.02, 130.65, 129.36, 129.08, 128.77, 127.70, 125.88, 124.55, 123.42, 123.08, 121.01, 59.77, 52.73, 45.81; m.f.: $C_{25}H_{24}N_4O_4S$; Calcd. m.w.: 476.55; HRMS: 477.1610 $[M+H]^+$.

Biological assays: Chemicals, buffer solutions and agarose gel used in this study were sourced from Thermo-Fisher Scientific and Sigma-Aldrich, USA. Electrophoresis was performed using agarose gel containing 4% Tris-Borate-EDTA (TBE). Fluorescence emissions were analyzed and quantified with a double fluorescence FMYG100 microscope, while cytofluorometric analysis was conducted using a Beckman Coulter Gallios 10/3 Cytofluorometer.

Antibacterial activity: The *in vitro* antibacterial activity of synthesized derivatives **8a-l** was evaluated using the agar well diffusion method on Muller-Hinton agar. The strains of Gram-negative and Gram-positive bacteria *Escherichia coli* and *Corynebacterium*, respectively, were tested at concentrations of 25, 50, 75 and 100 µg/mL of the respective standards of streptomycin, chloramphenicol and tetracyclin at 100 µg/mL. The nutritional agar and agar plates were used to obtain 10^4–10^6 colony forming units (CFU) in median. A sterile cork borer was used to create an aseptic hole with a diameter of 6-8 mm and a spacing of 25 mm. A 10 µL of examined substances in DMSO was applied to each well and the plates were incubated at 37 ºC for 24 h. Visible inhibition zones around the wells indicated antibacterial activity, with the diameter of the zones indicating the level of bacterial growth inhibition. Agar dilution was used to determine the zone of inhibition values, representing the lowest concentration at which bacterial growth is inhibited.

Molecular docking: A study was conducted to understand the antibacterial mechanism and intermolecular interactions among small molecule compounds. The docking experiments were conducted using the molecular operating environment (MOE) software suite in 2015, using DNA gyrase A from *E. coli*. The crystal structure was sourced from the Protein Data Bank and the compounds were drawn using ChemDraw. The protein structure was corrected using the structure preparation wizard, adding hydrogen atoms, removing solvent molecules and performing energy minimization. The final structures were saved and the program requirements were set up, including dummy atoms as the docking site, triangle matcher for placement, London dG for scoring, stiff receptor for refining and GBVI/WSA dG for posture selection. MDB files for the three ligands were loaded and general dock calculations were performed automatically. After the docking steps were completed, the obtained poses were examined [18,19].

RESULTS AND DISCUSSION

Scheme-I describes the multi-step process for constructing new analogs, the most significant of which is DAS piperazineamide derivatives (**8a-l**). Synthesis of 2-phenylthioaniline (**3**) involved reacting thiophenol with 1-chloro-2-nitrobenzene, with some minor procedural modification and then reduction the resulting compound. Chloroacetylchloride was used in the subsequent procedures to produce acetamide of compound **4**. Further, compound **4** was piperazinated using Boc-protected piperazine, yielding compound **5**. The Boc protecting group was removed with TFA in DCM, yielding compound **6**. In turn, compound **6** was treated various aromatic carboxylic acids **7a-l**, resulting in the formation of DAS piperazine-amide analogues **8a-l**. The structures were confirmed through FT-IR, ^{1}H NMR, ^{13}C NMR and HR-MS spectral recordings.

Antibacterial activity: The diverse properties of the DAS piperazine-amide derivatives **8a-l** were investigated by determining their ability to inhibit both *Corynebacterium* (Gram positive) and *Escherichia coli* (Gram-negative) bacteria using a modified approach [20] streptomycin, tetracycline and chloramphenicol are used as standard drugs. The efficacy of the analogs was assessed through minimal inhibition zone (MIZ) values, as presented in Table-1.

The antibacterial activity of DAS piperazine-amide derivatives **8a-l** varied significantly, with MIZ values ranging from

TABLE-1
MINIMAL INHIBITION ZONES (MIZ) (mm) OF ANTIBACTERIAL ACTIVITY OF COMPOUNDS **8a-l** AGAINST TWO BACTERIAL STRAINS AT FOUR DIFFERENT CONCENTRATIONS

Strains	Gram-positive bacterium (*Corynebacterium*)					Gram-negative bacterium (*Escherichia coli*)				
	25 µL	50 µL	75 µL	100 µL	Standard drug	25 µL	50 µL	75 µL	100 µL	Standard drug
8a	11	13	14	18	23	10	12	14	16	26
8b	–	09	11	16	23	10	11	12	14	26
8c	10	14	16	19	23	11	14	15	17	26
8d	20	23	24	23	16	20	25	26	29	16
8e	10	12	13	17	16	–	12	13	15	16
8f	10	15	14	18	21	–	14	13	15	20
8g	22	23	22	23	21	15	19	18	21	20
8h	20	25	26	31	16	20	25	27	29	16
8i	16	17	21	24	22	14	19	16	21	28
8J	16	18	20	21	16	14	16	16	20	16
8k	19	25	25	25	17	22	24	24	27	16
8l	16	20	21	23	17	14	18	20	24	16

Standard antibiotic drugs: Streptomycin: **8a**, **8b** and **8c**, Tetracyclin: **8e**, **8i** and **8l**, Chloromphenicol: **8d**, **8f**, **8g**, **8h**, **8j** and **8k**

9 to 31 mm at concentrations of 25, 50, 75 and 100 µL. Notably, compound **8h** (3,4-dinitrobenzene) showed significant antibacterial activity, with MIZ values of 20, 25, 26 and 31 against Gram-positive bacterium and 20, 25, 27 and 29 against Gram-negative bacterium at the same concentrations. Also, nitro substituent carboxamide analogues **8h**, **8d** and **8l** exhibited strong antibacterial action against both bacterial species. When examining the position of nitro substituent, a shift from position **8d** (4-nitro, *para*) to **8l** (3-nitro, *meta*) resulted in diminished inhibitory activity. However, the disubstituted compound **8h** (3,4-dinitro) maintained significant antibacterial action against the tested microorganisms. Moreover, moving the chlorine substituent from the *para* position in compound **8a** to the *ortho* position in compound **8i** enhanced its effectiveness.

The introduction of another chlorine atom into the phenyl ring from compound **8a** or **8i** to compound **8j**, which displayed superior antibacterial activity compared to standard antibiotics. Similarly, compounds **8k** and **8i**, featuring iodine and chlorine groups respectively in the *ortho* positions of their aryl carboxamide structures, showed comparable inhibitory effects on the tested bacteria. In contrast, *para*-substituted compounds, such as **8e** (4-fluoro), **8a** (4-chloro) and **8b** (4-bromo), exhibited lower potency overall. Hence, phenyl rings with dual substituents, including compound **8h** (3,4-dinitro), compound **8j** (2,4-dichloro), compound **8f** (4-hydroxy,3-methoxy) and compound **8c** (3,4-dimethoxy), displayed substantial effectiveness against both Gram-positive and Gram-negative bacteria.

Remarkably, with the exception of compounds **8a**, **8b**, **8c** and **8f**, all target compounds outperformed the standard antibiotics streptomycin, chloramphenicol and tetracycline. The active analogs **8h**, **8d**, **8k** and **8j** demonstrated a strong preference for inhibiting both bacterial types, with inhibition zones ranging from 9 to 31 mm, highlighting their activity as potent antibacterial agents.

The investigation of DAS piperazine-amide derivatives **8a-l** highlights those compounds with disubstituted phenyl rings exhibit significantly enhanced antibacterial activity compared to monosubstituted ones. Remarkably, derivatives **8h** (3,4-dinitro), **8j** (2,4-dichloro) **8f** (4-hydroxy,3-methoxy) and compound **8c** (3,4-dimethoxy) showed remarkable effectiveness against both Gram-positive (*Corynebacterium*) and Gram-negative (*Escherichia coli*) bacteria.

Structure-activity relationship (SAR) analysis emphasized that the position of substituents is crucial; *ortho*-substituted compounds, such as **8i** and **8j**, demonstrated superior antibacterial potency compared to their *para*-substituted analogs, **8a** (4-chloro) and **8e** (4-fluoro). This underscores the significance of substituent placement in optimizing the antibacterial properties of these derivatives, suggesting that strategic modifications in their chemical structure can yield more potent antibacterial agents. These findings indicated that disubstituted compounds are particularly promising for further development in combating bacterial infections.

Molecular docking: This section presents an analysis of the interactions between the ligand elatine and key amino acids within the DNA gyrase binding site. The residues involved include serine (SER 116), threonine (THR 219), glutamine (GLN 267) and several others. The docked structure revealed various types of interactions, including hydrogen bonds, van der Waals forces and π-H interactions, as illustrated in Tables 2 and 3. These interactions suggest that hydrophilic fragments, such as asparagine (Asn) and glutamine (Gln), play critical roles in the binding affinity of the synthesized compounds to DNA gyrase (Fig. 2). Additionally, the observed inhibitory effects against bacterial growth may be linked to the disruption of the peptidoglycan layer in the bacterial cell wall. Overall, these findings indicated that the synthesized compounds could have significant implications for biological efficacy.

The molecular docking studies of synthesized piperazine-amide hybrids against the DNA GyraseA enzyme revealed significant insights into their potential antibacterial efficacy, especially compared to conventional antibiotics like streptomycin, ciprofloxacin, tetracycline and chloramphenicol. Among the tested compounds, **8h** (3,4-dinitro) exhibited the highest binding affinity of -7.58 kcal/mol, interacting with the crucial residues Asn 269 and Gln 267, which suggests a robust mech-

TABLE-2
MOLECULAR INTERACTION OF COMPOUNDS WITH DNA Gyr.A OF BACTERIA
BINDING AFFINITY SCORES, MOLECULAR INTERACTION AND BOND LENGTH

Compound	Substituent	Bond length (Å)	Binding affinity (Kcal/mol)	DNA Gyrase binding site residue
8a	4-Cl	3.51	-6.62	Ser 116
8d	4-NO_2	3.06, 3.01	-6.93	Thr 219, Gln 267
8f	4-OH, 3-OMe	2.66, 3.73	-7.24	Phe 96, Phe 96
8g	4-NH_2	2.84, 3.79, 3.25	-7.04	Phe 96, Ala 117, Gln 267
8h	3,4-di-NO_2	2.83, 3.63	-7.58	Asn 269, Gln 267
8i	2-Cl	3.26, 4.08	-7.10	Arg 91, Asn 269
8j	2,4-di-Cl	3.54	-7.14	Ile 112
8k	2-I	3.37, 3.45, 3.05, 4.18	-6.63	Ser 116, Ala 117, Gly 114, Asn 269
Streptomycin		2.72, 2.93, 2.81, 3.17, 2.93, 2.97	-7.38	GLY 114, ASP 87, SER 111, ASP 115, PHE 96, GLN 94
Ciprofloxacin		3.49	-5.10	ARG 91
Tetracycline		3.40, 3.09, 2.86	-5.80	PHE 96, GLN 94, ARG 91
Chloramphenicol		3.01, 3.12	-5.73	ALA 117, ARG 91

TABLE-3
MOLECULAR DOCKING ENERGIES (Kcal/mol)
OF THE TESTED LIGANDS

Compound	rsmd_refine	E_conf	E_refine
8a	0.9314	114.4180	-35.4377
8d	1.3732	144.2677	-37.3780
8f	1.7685	113.5544	-38.0758
8g	1.3779	84.6165	-38.2957
8h	1.2015	107.9662	-41.4197
8i	0.8842	96.3605	-41.3973
8j	1.1262	94.5075	-39.1546
8k	0.7902	106.6235	-35.9673
Streptomycin	1.3066	-105.2598	-38.8258
Ciprofloxacin	1.1013	128.4994	-16.8805
Tetracycline	1.3439	-17.5973	-29.8420
Chloramphenicol	1.1725	100.3267	-27.6884

rmsd_refine, the root-mean-squared-deviation (RMSD) between the heavy atoms of the predicted pose (after refinement) and those of the crystal structure (before refinement), E_conf, conformer energy in kcal/mol, E_refine, the score of refinement step of ligand conformer

anism for inhibiting the enzyme essential for bacterial DNA replication. The strong interaction is supported by a relatively low RMSD value of 1.2015, indicating stable binding.

Following closely, **8f** (4-OH, 3-OMe) achieved a binding affinity of -7.24 kcal/mol through interactions with Phe 96, further underscoring its potential as an effective antibacterial agent. Despite a higher RMSD of 1.7685, which may indicate a less optimal binding conformation, its affinity positions it favourably among the synthesized compounds. Similarly, **8j** (2,4-di-Cl) displayed binding affinities of -7.14 kcal/mol, respectively, engaging with Ile 112, suggesting that electronic properties of the substituents play a significant role in enhancing binding interactions and consequently, antibacterial efficacy. Also, **8d** (4-NO_2) displayed binding affinities of -6.93 kcal/mol, engaging with Thr 219, suggesting that electronic properties of the substituents play a significant role in enhancing binding interactions and, consequently, the antibacterial efficacy. Compound **8i** (2-Cl), with a binding affinity of -7.10 kcal/mol,

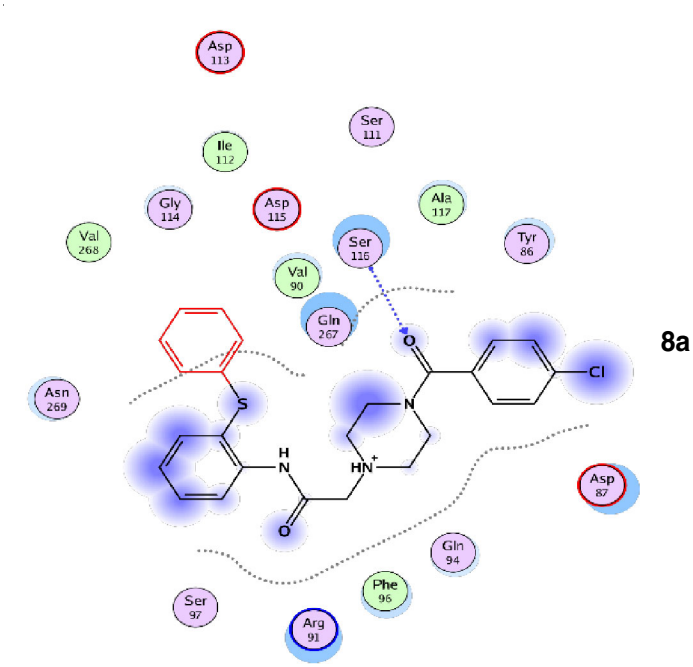

8a

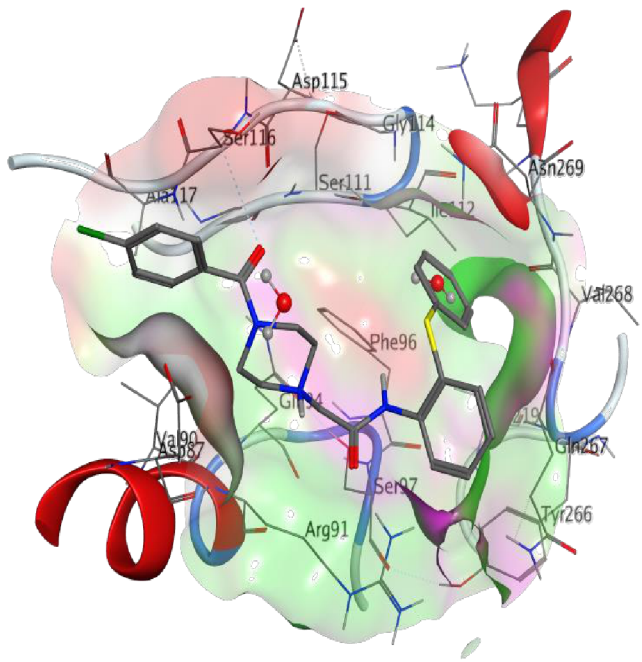

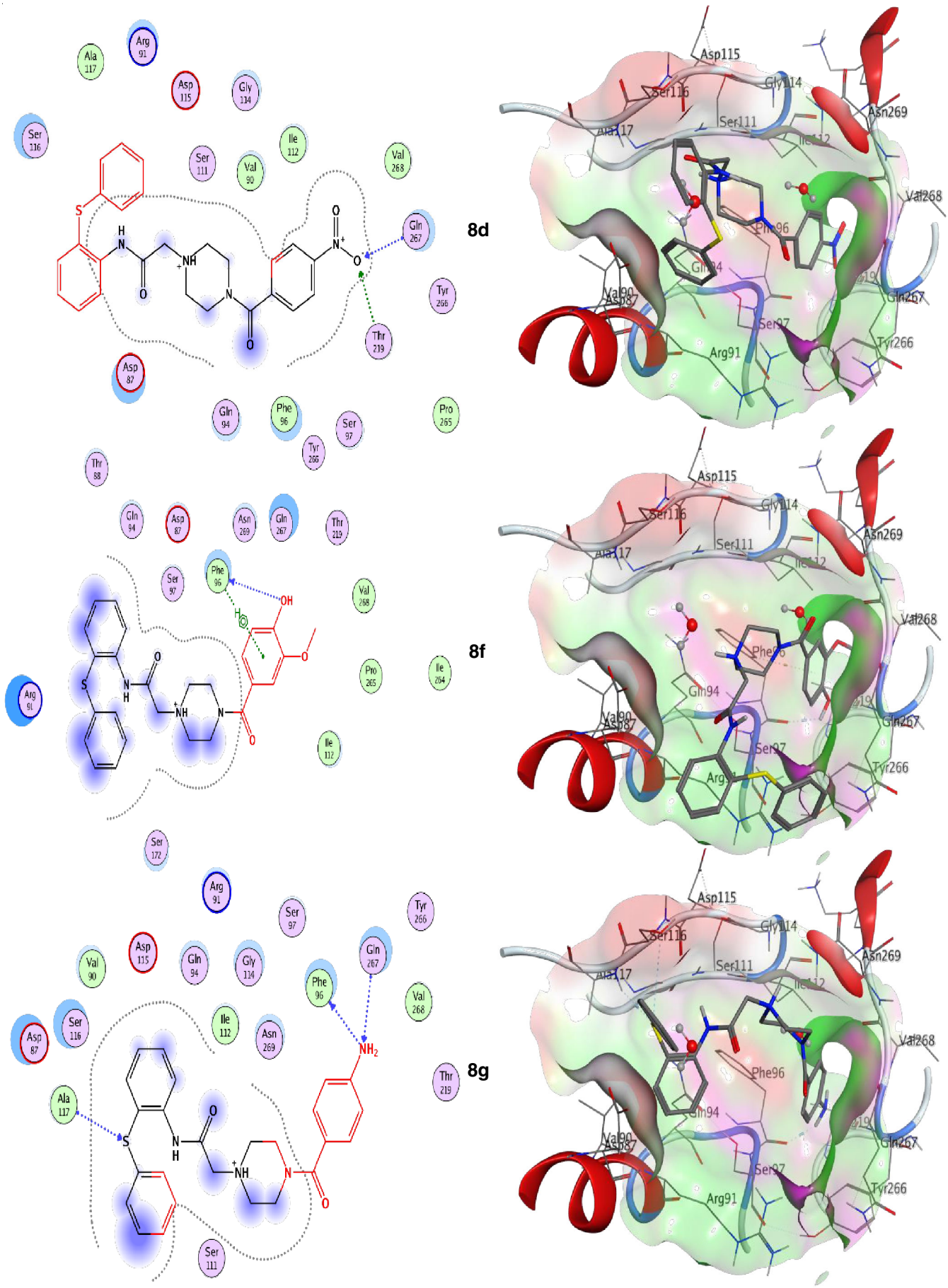
8d
8f
8g
Asp115
Gly114
Ser116
Ser111
Asn269
Val268
Phe96
Gln94
Val90
Asp87
Ser97
Tyr266
Arg91
Gln267

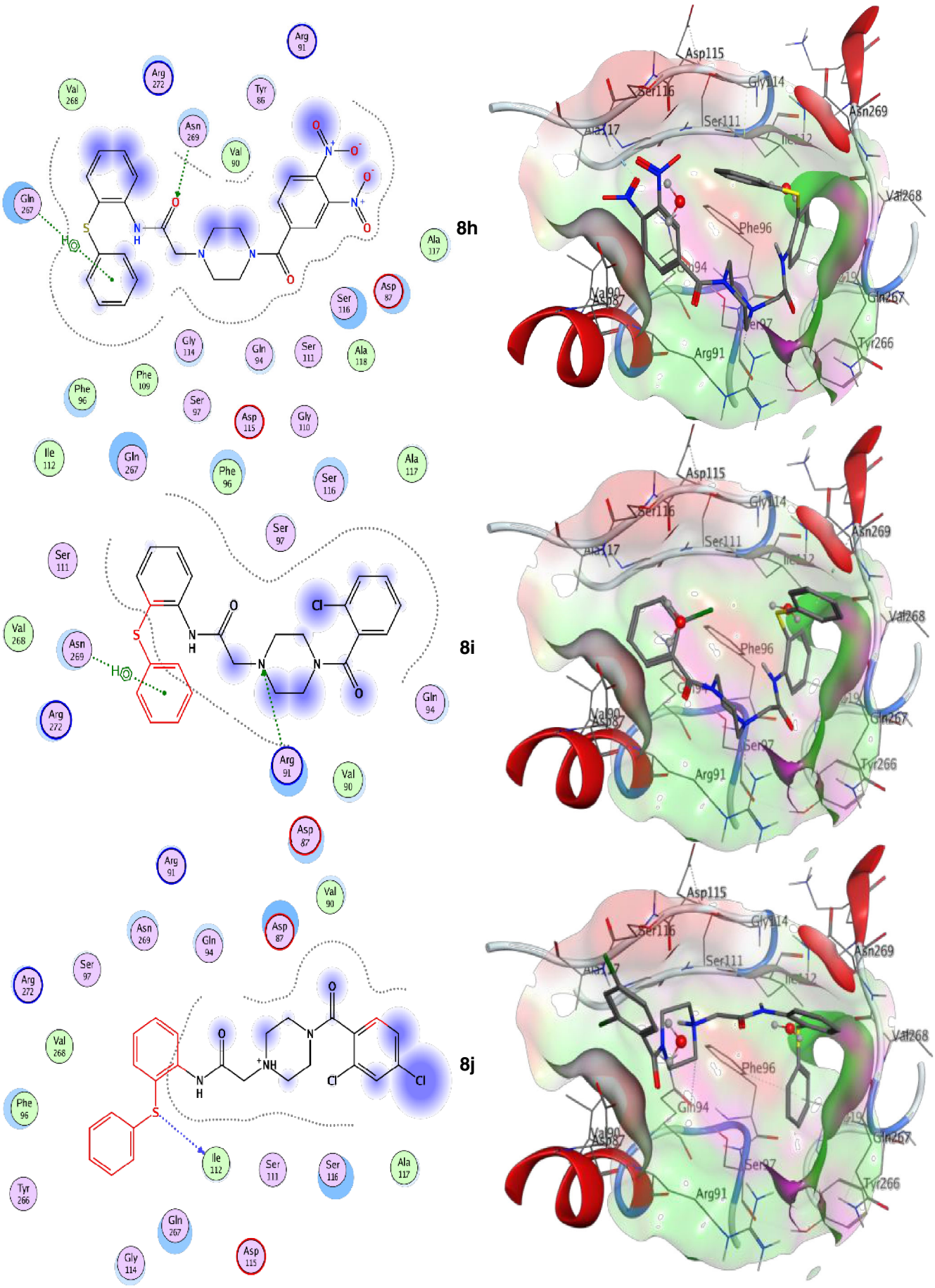
8h
8i
8j
Arg 91
Arg 272
Val 268
Tyr 86
Asn 269
Val 90
Gln 267
Ala 117
Asp 87
Ser 116
Gly 114
Gln 94
Ser 111
Ala 118
Phe 109
Phe 96
Ser 97
Asp 115
Gly 110
Ile 112
Cl
Asp115
Ser116
Gly114
Ser111
Asn269
Val268
Phe96
Gln94
Val90
Asp87
Ser97
Arg91
Tyr266
Gln267

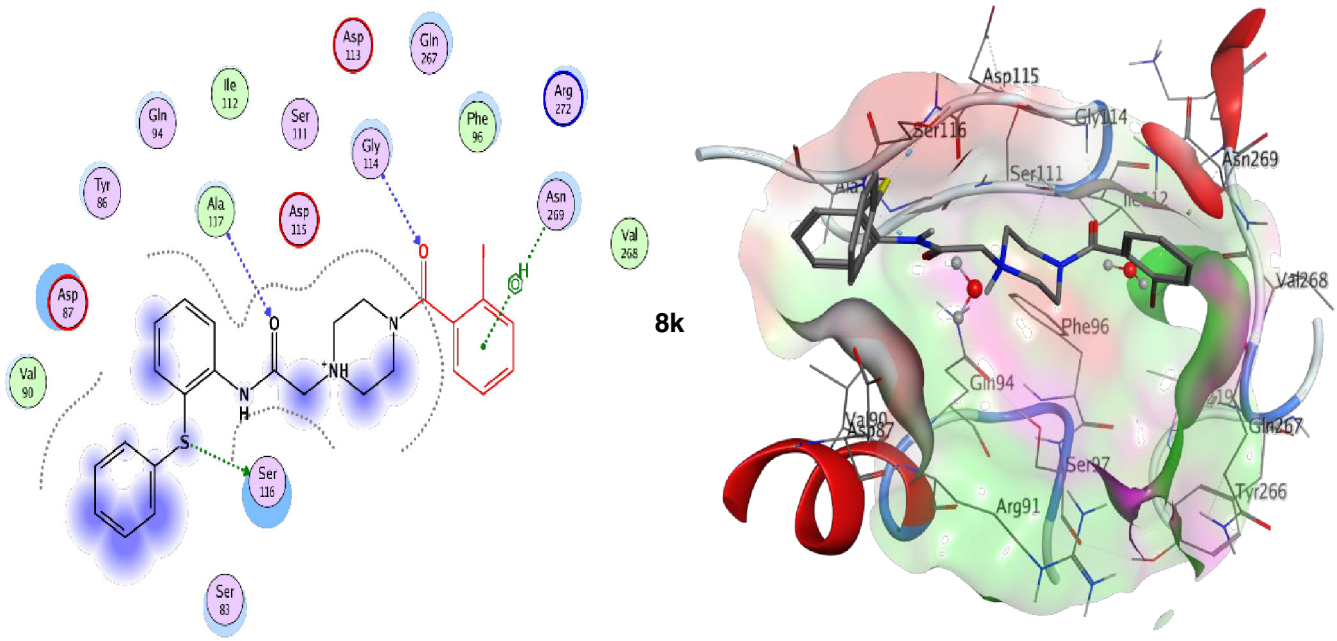

Fig. 2. The 2D & 3D binding modes of compounds **8a**, **8d**, **8f**, **8g**, **8h**, **8i**, **8j** and **8k** in the active site of DNA gyrase

interacted with Arg 91 and Asn 269, indicating that halogen substituents contribute positively to binding, whereas **8g** (4-NH_2) and **8a** (4-Cl) demonstrated moderate affinities of -7.04 kcal/mol and -6.62 kcal/mol, respectively, reflecting the importance of steric and electronic factors in their interactions. The compounds rmsd values, notably lower for **8k** (2-I) at 0.7902, support the idea that stable binding correlates with higher efficacy.

The observed structure-activity relationships (SARs) suggest that the introduction of electron-withdrawing groups and optimal steric configurations enhances the binding strength, leading to the improved antibacterial activity. Overall, these findings indicate that the synthesized DAS piperazine-amide hybrids hold promise as effective alternatives in combating resistant bacterial strains, warranting further investigation into their biological mechanisms and therapeutic applications.

Conclusion

The diarylsulfide (DAS) piperazine-amide derivatives **8a-l** were successfully synthesized and characterized, revealing their potential as antibacterial agents. The characterization techniques such as FT-IR, ^{1}H NMR, ^{13}C NMR and HR-MS confirmed the compounds chemical structures. Antibacterial testing against Gram-positive (*Corynebacterium*) and Gram-negative (*Escherichia coli*) bacteria showed MIZ values ranging from 9 to 31 mm, indicating varied efficacy. Structure-activity relationship (SAR) analysis revealed that disubstituted compounds, particularly **8h** (3,4-dinitro) and **8j** (2,4-dichloro), exhibited superior antibacterial activity. The positioning of substituents was crucial, with *ortho*-substituted compounds performing better than *para*-substituted ones. Molecular docking studies indicated that compound **8h** had the highest binding affinity (-7.58 kcal/mol) to the DNA gyrase enzyme, interacting with essential residues critical for bacterial DNA replication. This strong binding, alongside favourable rmsd values, suggesting that the compounds could effectively inhibit DNA gyrase. Finally, the synthesized DAS piperazine-amide derivatives demonstrate significant antibacterial properties, particularly those with multiple substituents that enhance binding affinity. Strategic structural modifications could lead to more potent agents, making them promising alternatives to conventional antibiotics, especially against resistant bacterial strains.

ACKNOWLEDGEMENTS

One of the authors, K. Sajitha, express her sincere thanks to UGC-New Delhi for the research grant UGC Letter No. F.25-1/2014-15(BSR)/7-187/2007 and also authors express their gratitude to Department of Microbiology, Yogi Vemana University, Kadapa for supporting antibacterial activity. Furtherly, authors express their gratitude to the Department of Chemistry, University of Hyderabad for providing the molecular docking study.

CONFLICT OF INTEREST

The authors declare that there is no conflict of interests regarding the publication of this article.

REFERENCES

1. L. Narendrakumar, M. Chakraborty, S. Kumari, D. Paul and B. Das, *Front. Microbiol.*, **13**, 1092556 (2023); https://doi.org/10.3389/fmicb.2022.1092556
2. X. Lin and U. Kück, *Appl. Microbiol. Biotechnol.*, **106**, 8007 (2022); https://doi.org/10.1007/s00253-022-12272-8
3. S.J. Dancer, *J. Antimicrob. Chemother.*, **48**, 463 (2001); https://doi.org/10.1093/jac/48.4.463
4. R.W. Jadhav, M. Al Kobaisi, L.A. Jones, A. Vinu and S.V. Bhosale, *ChemistryOpen*, **8**, 1154 (2019); https://doi.org/10.1002/open.201900193
5. F. von Nussbaum, M. Brands, B. Hinzen, S. Weigand and D. Häbich, *Angew. Chem. Int. Ed.*, **45**, 5072 (2006); https://doi.org/10.1002/anie.200600350

6. A.B. Shaik, R.R. Bhandare, S. Nissankararao, S. Shahanaaz, B.V.S. Lokesh and M.M. Rahman, *Arab. J. Chem.*, **14**, 102915 (2021); https://doi.org/10.1016/j.arabjc.2020.102915
7. R. Domalaon, G. G. Zhanel and F. Schweizer, *Curr. Top. Med. Chem.*, **16**, 1217 (2016); https://doi.org/10.2174/1568026615666150915112459
8. R.R. Bhandare, C. S.Munikrishnappa, G.V. Suresh Kumar, S.K. Konidala, D.K. Sigalapalli, Y. Vaishnav, S. Chinnam, H. Yasin, A.A. Al-Karmalawy and A.B. Shaik, *J. Saudi Chem. Soc.*, **26**, 1 (2022); https://doi.org/10.1016/j.jscs.2022.101447
9. F. Abedinifar, S. Bahadorikhalili, B. Larijani, M. Mahdavi and F. Verpoort, *Appl. Organomet. Chem.*, **36**, e6482 (2022); https://doi.org/10.1002/aoc.6482
10. A. Rosas-Hernández, C. Steinlechner, H. Junge and M. Beller, *Top. Curr. Chem.*, **376**, 1 (2018); https://doi.org/10.1007/s41061-017-0179-7
11. D.B. Janakiramudu, D.S. Rao, K. Madhu, G. Madhava, C.N. Raju and P.V. Chalapathi, *Org. Commun.*, **10**, 201 (2017); https://doi.org/10.25135/acg.oc.19.16.12.455
12. J. Vercouillie, S. Mavel, L. Galineau, T. Ragusa, R. Innis, M. Kassiou, S. Chalon, F. Dollé, J.-C. Besnard, D. Guilloteau and P. Emond, *Bioorg. Med. Chem. Lett.*, **16**, 1297 (2006); https://doi.org/10.1016/j.bmcl.2005.11.066
13. M. Asif, *Int. J. Adv. Sci. Res.*, **1**, 5 (2015); https://doi.org/10.7439/ijasr.v1i1.1766
14. C.P. Meher, A.M. Rao and M. Omar, *Asian J. Pharm. Sci. Res.*, **3**, 43 (2013).
15. M. Tugrak, H.I. Gul, K. Bandow, H. Sakagami, I. Gulcin, Y. Ozkay and C.T. Supuran, *Bioorg. Chem.*, **90**, 103095 (2019); https://doi.org/10.1016/j.bioorg.2019.103095
16. H.A. Saadeh, I.M. Mosleh and M.S. Mubarak, *Molecules*, **14**, 1483 (2009); https://doi.org/10.3390/molecules14041483
17. T. Khan, K. Sankhe, V. Suvarna, A. Sherje, K. Patel and B. Dravyakar, *Biomed. Pharmacother.*, **103**, 923 (2018); https://doi.org/10.1016/j.biopha.2018.04.021
18. R.K. Thalji, K. Raha, D. Andreotti, A. Checchia, H. Cui, G. Meneghelli, R. Profeta, F. Tonelli, S. Tommasi, T. Bakshi, B.T. Donovan, A. Howells, S. Jain, C. Nixon, G. Quinque, L. McCloskey, B.D. Bax, M. Neu, P.F. Chan and R.A. Stavenger, *Bioorg. Med. Chem. Lett.*, **29**, 1407 (2019); https://doi.org/10.1016/j.bmcl.2019.03.029
19. T. Khan, K. Sankhe, V. Suvarna, A. Sherje, K. Patel and B. Dravyakar, *Biomed. Pharmacother.*, **103**, 923 (2018); https://doi.org/10.1016/j.biopha.2018.04.021
20. D. Rajasekhar, D. Srinivasulu, C. Sridhar, G.V.N. Kumar and P. Ramesh, *J. Chin. Chem. Soc.*, **63**, 267 (2016); https://doi.org/10.1002/jccs.201500143